0013-7227/04/$15.00/0
Printed in U.S.A.

Endocrinology 145(11):5305–5312

doi: 10.1210/en.2004-0392

Oxidative Stress, β-Cell Apoptosis, and Decreased Insulin Secretory Capacity in Mouse Models of Hemochromatosis

ROBERT C. COOKSEY, HANI A. JOUIHAN, RICHARD S. AJIOKA, MARK W. HAZEL, DEBORAH L. JONES, JAMES P. KUSHNER, AND DONALD A. MCCLAIN

Research Service of the Veterans Affairs Medical Center (R.C.C., D.A.M.), and Departments of Medicine and Biochemistry, University of Utah School of Medicine (R.C.C., H.A.J., R.S.A., M.W.H., D.L.J., J.P.K., D.A.M.), Salt Lake City, Utah 84132

The pathogenesis of diabetes associated with hemochromatosis is not known. We therefore examined glucose homeostasis and β-cell function in mouse models of hemochromatosis. Mice with targeted deletion of the hemochromatosis gene (*Hfe*$^{-/-}$) on the 129/Sv genetic background exhibited a 72% increase in iron content in the islets of Langerhans compared with wild-type controls. Insulin content was decreased in *Hfe*$^{-/-}$ mice by 35%/pancreas and 25%/islet. Comparable decreases were seen in the mRNA levels of β-cell-specific markers, ins1, ins2, and glucose transporter 2. By 6–8 months, islets from *Hfe*$^{-/-}$ mice were 45% smaller, associated with increased staining for activated caspase 3 and terminal deoxynucleotidyl transferase-mediated deoxy-UTP nick end labeling. Islets from *Hfe*$^{-/-}$ mice were also desensitized to glucose, with half-maximal stimulation of insulin secretion seen at 16.7 ± 0.9 mM glucose in perifused islets from *Hfe*$^{-/-}$ mice compared with 13.1 ± 0.6 mM glucose in wild-type animals. Carbonyl protein modification, a marker for oxidative stress, was increased by 58% in Hfe$^{-/-}$ islets. Despite decreased islet size, *Hfe*$^{-/-}$ mice exhibited enhanced glucose tolerance. Fasting serum insulin levels were comparable between *Hfe*$^{-/-}$ and *Hfe*$^{+/+}$ mice, but were 48% lower in the *Hfe*$^{-/-}$ mice 30 min after challenge. Similar results were seen in mice carrying an *Hfe* mutation analogous to the common human mutation (C282Y) and in mice fed excess dietary iron. *Hfe*$^{-/-}$ mice on the C57BL6 background exhibited decreased glucose tolerance at 10–12 months due to an inability to increase insulin levels as they aged. We conclude that iron excess results in β-cell oxidant stress and decreased insulin secretory capacity secondary to β-cell apoptosis and desensitization of glucose-induced insulin secretion. This abnormality alone, however, is insufficient to cause diabetes. (*Endocrinology* 145: 5305–5312, 2004)

HEREDITARY HEMOCHROMATOSIS type 1 is transmitted as an autosomal recessive trait and occurs at a frequency of approximately five per 1000 in populations of northern European extraction (1, 2). Most patients with hemochromatosis are homozygous for a single nucleotide substitution in the hemochromatosis gene (*Hfe*), resulting in a change from cysteine to tyrosine at amino acid 282 in the Hfe protein (C282Y) (3). The *Hfe* gene is located near the human leukocyte antigen A locus, and encodes a 343-amino acid protein (Hfe) that has a wide tissue expression and is involved in the regulation of gastrointestinal iron absorption, although the precise mechanism of its action remains unknown. The Hfe protein exists as a heterodimer with β_2-microglobulin that binds to and reduces the affinity of the transferrin receptor for iron-saturated transferring (4). Phenotypic expression of hemochromatosis may vary from a fully penetrant clinical syndrome (skin pigmentation, cirrhosis, arthritis, endocrinopathy, and cardiomyopathy) to a simple laboratory abnormality, namely an elevated transferrin saturation without organ injury (1, 5). There is an increasing appreciation, however, that significant morbidity may be present in the affected population even before clinical presentation (6).

Although diabetes is part of the classic presentation of hemochromatosis, little is known about its pathogenesis. It is assumed, but unproven, that excess iron stores are directly responsible for the diabetes. The relative contributions of insulin deficiency, hepatic dysfunction, and insulin resistance to hemochromatosis-associated diabetes, however, are not known. We have therefore examined insulin secretory capacity in mouse models of hemochromatosis and mice with dietary iron overload. Our results demonstrate that iron overload in the β-cell results in decreased insulin secretion secondary to β-cell apoptosis, loss of β-cell mass, and desensitization of glucose-induced insulin secretion. These defects alone, however, are well compensated and not sufficient to cause diabetes.

Materials and Methods

Experimental animals

Mice were of the 129/SvEvTac and C57BL6 genetic background. Targeted mutagenesis was used to produce a knockout (*Hfe*$^{-/-}$) and the equivalent C282Y mutation (*Hfe*$^{y/y}$) in the mouse (7, 8). The mutation was bred onto the appropriate background for at least eight generations. Dietary iron overload was produced by supplementing the diet of wild-type mice with 20 g/kg carbonyl iron (Teklad TD91013, Harlan, Indianapolis, IN). The control diet contained 0.33 g/kg iron (TD8640). Age- and sex-matched wild-type 129/SvEvTac (*Hfe*$^{+/+}$) and C57 (*Hfe*$^{+/+}$) mice were used as controls. Procedures were approved by the institutional animal care and use committee of University of Utah.

Abbreviations: AIRg, Acute insulin response to glucose; GLUT, glucose transporter; HBSS, Hanks' balanced salt solution; IPGTT, ip glucose tolerance testing; PPARα, peroxisomal proliferator-activated receptor α; TUNEL, terminal deoxynucleotidyl transferase-mediated deoxy-UTP nick end labeling.

***Endocrinology* is published monthly by The Endocrine Society (http://www.endo-society.org), the foremost professional society serving the endocrine community.**

Islet isolation

Islets were isolated using the intraductal Liberase RI digestion technique as described previously (9). Briefly, mice were killed by cervical dislocation, and 3 ml Hanks' balanced salt solution (HBSS) containing 0.3 mg/ml Liberase RI Purified Enzyme Blend (Roche, Indianapolis, IN) were injected into the pancreas through the bile duct. Pancreata were excised and incubated at 37 C for 12 min, briefly shaken, and filtered through a nylon mesh. The islets were then further purified by hand-picking under a dissecting microscope to eliminate any remaining exocrine tissue.

Perifusion studies

Islets were perifused as previously described (10, 11). Briefly, size-matched islets (13–16/study) were isolated and placed on a 62-μm monofilament nylon mesh (Small Parts, Inc., Miami Lakes, FL) inside a 13-mm filter holder (Swinnex, Millipore Corp., Bedford, MA). For basal insulin secretion, islets were perifused in Krebs-Ringer bicarbonate buffer containing 3 mM glucose, 1 mg/ml BSA, 10 mM HEPES (pH 7.3), 1× MEM amino acid solution, 1× MEM nonessential amino acid solution (Invitrogen Life Technologies, Inc., Grand Island, NY), and 5 mM $NaHCO_3$ at a flow rate of 1 ml/min for 30 min before collection of fractions. The Krebs-Ringer bicarbonate buffer was maintained at 37 C in a water bath and was gassed with 95% O_2/5% CO_2. After the first 30-min period, glucose concentrations perifusing the islets were increased to a final concentration of 35 mM over a period of 100 min using a linear gradient. Fractions (1 ml) of perifusion buffer containing glucose and the released insulin were collected at 1-min intervals. Glucose levels were measured using a Glucose Analyzer 2 (Beckman Instruments, Inc., Fullerton, CA). Insulin levels were assessed by RIA (Sensitive Rat Insulin RIA Kit, Linco Research, Inc., St. Charles, MO).

Determination of tissue iron levels in liver and islets

Iron content was measured on acid hydrolysates of tissue by either atomic absorption spectroscopy or a colorimetric assay (12). Approximately 100 mg liver or 150 islets were used for iron measurements.

Histology and determination of β-cell mass

For terminal deoxynucleotidyl transferase-mediated deoxy-UTP nick end labeling (TUNEL) and caspase 3 immunohistochemistry, pancreata (six per group) were fixed in 10% formalin and paraffin-imbedded, and 10-μm serial sections were collected. DNA fragmentation analysis was performed using TUNEL according to manufacturer's protocol (*In Situ* Cell Death Detection Kit, Roche, Nutley, NJ) (13) with slight modification. Briefly, sections were deparaffinized and blocked in 3% H_2O_2/PBS solution for 5 min at room temperature. Samples were then placed in 10 ml 0.1 M citrate buffer, pH 3.0, and subjected to microwave irradiation at 770 watts for 5 min, followed by a 15-min cooling period. Samples were then washed twice with PBS, incubated in permeabilization solution (0.1% Triton X-100 in 1× PBS) for 2 min on ice, and finally washed twice with PBS. Tissue sections were incubated for 15 min at room temperature with proteinase K (20 μg/ml) working solution. Samples were then blocked for 30 min at room temperature with 20% bovine serum and 3% BSA in PBS, treated with TUNEL reaction mix for 1 h at 37 C, washed in PBS, and blocked again in 20% normal sheep serum, 3% BSA, and 1% (wt/vol) Roche Blocking reagent for 30 min at room temperature. Signal conversion was accomplished by incubating slides in 50 μl Converter-POD solution (1:3 anti-fluorescein antibody conjugated with horseradish peroxidase), followed by washing with PBS. Finally, 3,3′-diaminobenzidine substrate solution was applied for 30 sec, reactions were stopped with dH_2O, and tissue sections were counterstained with hematoxylin and visualized under the light microscope.

Sections for analysis of activated caspase 3 were deparaffinized, rehydrated, treated with 3% H_2O_2, and blocked with 5% horse serum in HBSS, followed by treatment with cleaved caspase 3 primary antibody (Cell Signaling Technology, Beverly, MA) and donkey antirabbit secondary antibody (Jackson ImmunoResearch Laboratories, West Grove, PA). Four slides per pancreas with an average of 10 islets/slide were scored in a blinded fashion.

For determination of islet size, deparaffinized sections (10 μm/section, three pancreata per group) were treated with antiglucagon (1:100; Novacastra/Vector Laboratories, Inc., Burlingame, CA), followed by antirabbit 488 AlexaFluor (1:1000; Molecular Probes, Eugene, OR). After washing with PBS, sections were treated with antiinsulin (DakoCytomation, Carpinteria, CA), followed by antiguinea pig 594 AlexaFluor (Molecular Probes; 1:1000). Fluorescent confocal images were captured, and surface area analysis was performed using Velocity software (version 2.01, Improvision, Lexington, MA). Fifty to 100 islets/pancreas were analyzed in a blinded fashion.

Total pancreatic and islet insulin content

Pancreata (five mice per group; 6–8 months old) were extracted in acid-ethanol (14). Size-matched islets (5–10/determination) from each group were sonicated in 1 ml HBSS at setting 4 for 10 1-sec bursts (Brinkmann Sonic Dismembrator 60, Fisher Scientific, Pittsburgh, PA). Insulin was measured using the Sensitive Rat Insulin RIA Kit (Linco Research, Inc.).

Intraperitoneal glucose tolerance testing (IPGTT) and acute insulin secretory responses in vivo

Experimental animals were fasted for 6 h, after which glucose (1 g/kg body weight) was administered ip to nonsedated animals. Tail vein blood (3 μl) was sampled for glucose determination (Glucometer Elite, Bayer Corp., Tarrytown, NY) before and 15, 30, 60, 90, and 120 min after glucose administration. Tail vein blood (50 μl) was also collected for insulin determination before and 30 min after the start of the IPGTT.

Intraperitoneal insulin tolerance test

Human recombinant insulin (Eli Lilly & Co., Indianapolis, IN; 0.75 U/kg body weight) was administered ip to fed conscious mice. Tail vein blood (3 μl) was sampled for glucose determination (Glucometer Elite, Bayer Corp.) before and 15, 30, 60, 90, 120, 150, and 180 min after insulin administration.

Quantitation of transcript levels by RT-PCR

After a 24-h fast, mice were killed, and the pancreata were dissected, weighed, submerged in 800 μl RNA-Later (Ambion, Austin, TX), and stored at −20 C. Each whole pancreas was then submerged in 1.0 ml Tri-Reagent (MRC, Cincinnati, OH)/50 mg pancreas tissue, homogenized as described above, and passed through a 20-gauge syringe. RNA extraction steps were performed according to the Tri-Reagent manufacturer's protocol (MRC). First strand cDNA synthesis was carried out using Moloney murine leukemia virus reverse transcriptase (Invitrogen Life Technologies, Inc., Carlsbad, CA) according to the manufacturer's protocol, with 3.0 μg whole pancreas RNA and 240 ng random hexamer primers (Invitrogen Life Technologies, Inc.) in a reaction volume of 20 μl.

Real-time PCR was performed with a rapid thermal cycler (LightCycler, Roche) as previously described (15). Primers were designed using Whitehead institute's Primer 3 software (http://frodo.wi.mit.edu/primer3/primer3_code.html). The primers used were: mouse insulin 1, 5′-CTGCTGGCCCTGCTTGC-3′ and 5′-GGGTCGAGGTGGGCCTT-3′, amplifying a 315-bp product; mouse insulin 2, 5′-CCTGCTGGCCCTGCTCTT-3′ and 5′-GGCTGGGTAGTGGTGGGTCTA-3′, amplifying a 325-bp product; glucose transporter-2 (GLUT2), 5′-TGTATCAGGACTGTATTGTGGGCTAAT-3′ and 5′-TGGTGACATCCTCAGTTCCTCTTAGT-3′, amplifying a 335-bp product; peroxisomal proliferator-activated receptor α (PPARα), 5′-TGCCTGTCTGTCGGGATGT-3′ and 5′-AATCGGACCTCTGCCTCTTTG-3′, amplifying a 335-bp product; and cyclophilin-A, 5′-AGCACTGGAGAGAAAGGATTTGG-3′ and 5′-TCTTCTTGCTGGTCTTGCCATT-3′, amplifying a 349-bp product. Reactions (10 μl) were performed using approximately 8 ng cDNA as template. Final concentrations of PCR reagents were 0.5 μM of each primer, 200 μM of each deoxy-NTP, 50 mM Tris (pH 8.3), 500 μg/ml nonacetylated BSA, 3.0 mM $MgCl_2$, 0.04 U/μl Platinum *Taq* DNA polymerase (Invitrogen Life Technologies, Inc.), and a 1:30,000 dilution of SYBR Green I fluorescent dye (Molecular Probes). The protocol (denaturation at 95 C for 0 sec; annealing at 62 C for 0 sec; elongation at 72 C for 12 sec) consisted of 40 cycles to ensure a linear range of the PCR. For each transcript, analyses of the melting curves and visualization after

agarose gel electrophoresis confirmed the absence of nonspecific products. Quantitation of cDNA products was accomplished by the LightCycler software, using the second derivative maximum or threshold cycle at which the fluorescence clearly increases above background fluorescence. Standard curves of log cDNA amount *vs.* crossing point cycle number were constructed for each run of the four transcripts of interest. Results for each sample were normalized by dividing the relative amount of each transcript by the relative amount of cyclophilin-A transcript (averaged from triplicate determinations) generated from that sample.

Determination of intracellular protein oxidation in pancreatic islets

Cell extracts were prepared from freshly isolated islets by incubation in 100 μl lysis buffer [50 mM Tris-HCl (pH 8.0), 150 mM NaCl, 10% (vol/vol) glycerol, 1% (vol/vol) Nonidet P-40, 1 mM NaF, 2 mM Na_3VO_4, 1 mM phenylmethylsulfonylfluoride, 1 mM EDTA, and protease inhibitor cocktail tablets; Roche]. Protein carbonyl content was measured according to manufacturer protocol (OxiBlot Protein Oxidation Detection Kit, Chemicon International, Temecula, CA). Briefly, protein samples (5 μg/lane) were derivatized with dinitrophenyl hydrazine, fractionated by 10% SDS-PAGE, and electroblotted to Immobilon-PSQ transfer membranes (Millipore Corp.). The derivatized proteins were sequentially reacted with rabbit antidinitrophenyl and horseradish peroxidase-conjugated goat antirabbit IgG antibodies and visualized by chemiluminescence (Amersham Bioscience, Little Chalfont, UK). Equal protein loading on gels was verified by Coomassie Blue staining. Densitometry measurements were obtained using a UMAX Astra 3450 scanner (UMAX Technologies, Fremont, CA) and NIH Image 1.63 (Bethesda, MD).

Statistical procedures

Descriptive statistics are represented as the average ± SE. A *t* test (two-tailed) was used to compare differences between experimental and control groups.

Results

Increased tissue iron concentrations in $Hfe^{-/-}$ mice

Iron concentrations were measured in liver and in pancreatic islets (100 islets/determination; three to five determinations per group). $Hfe^{-/-}$ mice had a 72% increase in the level of iron in the islets of Langerhans compared with controls (Fig. 1A; 0.055 ± 0.013 *vs.* 0.032 ± 0.009 pg/islet; $P < 0.05$). Hepatic iron was similarly elevated (Fig. 1B; 738 ± 22 *vs.* 171 ± 45 μg/wet weight; $P < 0.01$). The iron was elevated by 5 wk of age and remained elevated thereafter (not shown).

Decreased pancreatic and islet insulin content resulting from β-cell apoptosis and decreased β-cell mass

We next assessed the effect of iron accumulation on insulin content and β-cell mass. The total pancreatic insulin content (Fig. 2A, $P < 0.03$) and insulin content per islet (Fig. 2B; $P = 0.01$) were both lower in $Hfe^{-/-}$ mice at 6–8 months of age. The loss of insulin was paralleled by decreased mRNA levels in the total pancreas of the two rodent insulin genes, ins1 and ins2; the liver and β-cell-specific glucose transporter, GLUT2; and the nuclear receptor, PPARα. Ins1 and ins2 mRNA levels, normalized to total pancreatic cyclophilin-A, were decreased in $Hfe^{-/-}$ mice to 73% and 68%, respectively, of the levels in wild-type controls (Fig. 2C; $P = 0.0002$ for both ins1 and ins2). The mRNA for GLUT2 was decreased to 55% of the level in $Hfe^{+/+}$ mice ($P = 0.001$). PPARα mRNA was decrease by 24%, although this result was not statistically significant.

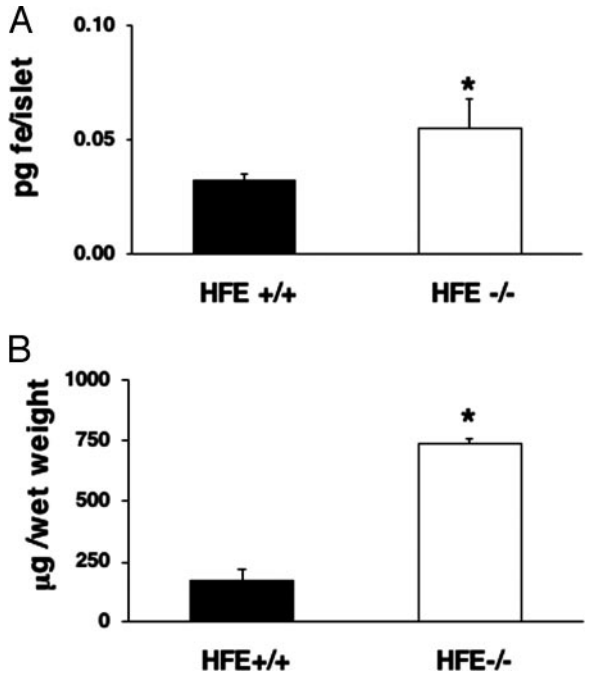

FIG. 1. Increased islet and hepatic iron content in $Hfe^{-/-}$ mice. Values are presented as the mean ± SE. A, Pancreatic islet iron levels in were significantly higher in 6- to 8-month-old $Hfe^{-/-}$ mice (0.055 ± 0.013 *vs.* 0.032 ± 0.009; *, $P < 0.05$). B, Hepatic iron content was significantly increased in $Hfe^{-/-}$ mice (738 ± 22 *vs.* 171 ± 45; *, $P < 0.01$).

These results suggest a general loss of β-cells in the iron-overloaded mice, and that was found to be the case. The $Hfe^{-/-}$ mice exhibited a 45% decrease in islet surface area compared with the control group (Fig. 3; $P = 0.02$). No change was noted in the numbers or distribution of α-cells, visualized by staining for glucagon (Fig. 3A). No lymphocytic infiltration of the islets was noted in stained sections (not shown).

Two markers for apoptosis were examined. β-Cells from $Hfe^{-/-}$ mice exhibited a 2.7-fold increase in staining for activated caspase 3 (Fig. 4A; $P = 0.02$) and a 1.6-fold increase in TUNEL staining (Fig. 4B; $P = 0.05$).

Decreased glucose sensitivity in $Hfe^{-/-}$ mice

To assess whether there were additional functional defects in glucose-induced insulin secretion, the glucose sensitivity of islets from 8-wk-old mice was determined. Islets were perifused with a linearly increasing gradient of glucose concentrations, and insulin was measured in the perifusate. Islets from the $Hfe^{-/-}$ mice were significantly less sensitive to glucose for stimulation of insulin secretion compared with control mice, as revealed by a rightward shift in the glucose dose-response curve. Half-maximal insulin secretion was seen at 16.7 ± 0.9 mM glucose in $Hfe^{-/-}$ islets compared with 13.1 ± 0.6 mM in wild-type islets (Fig. 5; $P < 0.006$). These results were confirmed by perifusion with static concentrations of glucose. Namely, $Hfe^{-/-}$ islets did not increase insulin secretion when the glucose concentration was increased from 3 to 5 mM, whereas wild-type islets exhibited an increase of 15% (not shown).

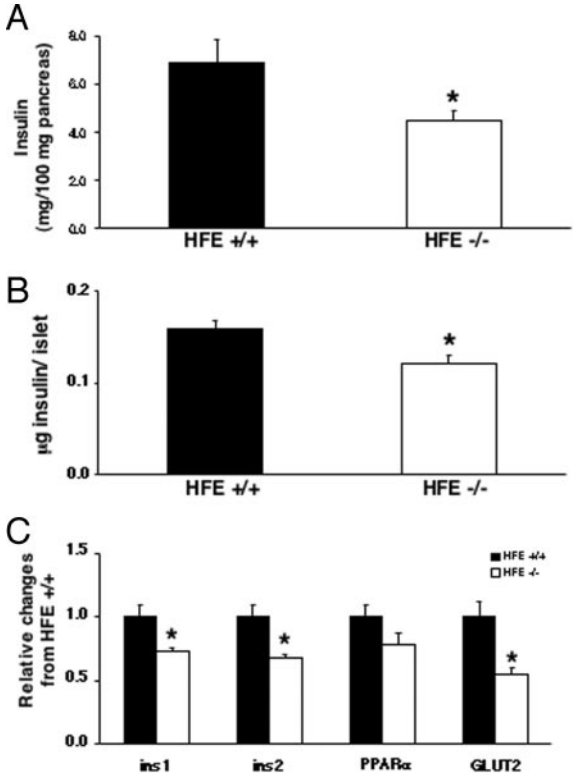

FIG. 2. Lower total pancreatic and islet insulin content, and decreased mRNAs for β-cell markers in age-matched (6–7 months old) and sex-matched (male) $Hfe^{-/-}$ mice and $Hfe^{+/+}$ controls. A, Pancreata were acid digested, and total insulin content was determined. Insulin content was significantly lower in the $Hfe^{-/-}$ mice (4.5 ± 0.7 *vs.* 6.9 ± 0.4 mg insulin/100 mg pancreas; n = 6/group; *, $P < 0.03$). There were no differences in body weight ($Hfe^{-/-}$, 21.1 ± 0.8; $Hfe^{+/+}$, 21.9 ± 0.7 g) or pancreatic weight ($Hfe^{-/-}$, 0.21 ± 0.01; $Hfe^{+/+}$, 0.24 ± 0.01 g) in these animals. B, Isolated islets from $Hfe^{-/-}$ mice contained significantly less insulin than controls (0.12 ± 0.01 *vs.* 0.16 ± 0.01 µg insulin/islet; 10–12 mice/group; *, $P < 0.01$). C, Lower expression of mRNAs for ins1 and ins2 (*, $P < 0.002$) and GLUT2 (*, $P < 0.001$) in $Hfe^{-/-}$ mice compared with wild-type controls. Values represent the percent change in $Hfe^{-/-}$ samples (n = 4 separate pancreata) compared with the $Hfe^{+/+}$ control samples (n = 4).

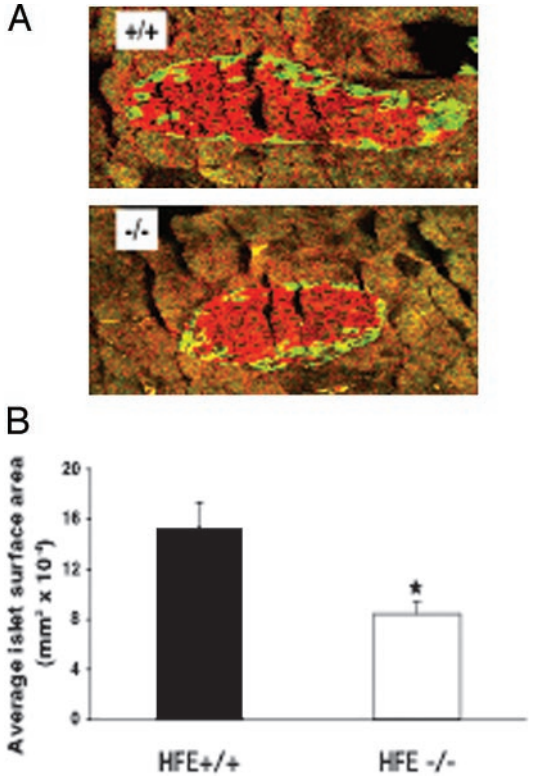

FIG. 3. Decreased islet size in $Hfe^{-/-}$ mice. A, Insulin (*red*) and glucagon (*green*) fluorescent immunostaining of pancreatic tissue from 8- to 10-month-old $Hfe^{+/+}$ and $Hfe^{-/-}$ mice. B, Decreased surface area of β-cells (*, $P = 0.042$; n = 4 animals/group; four to eight slides/animal, with at least 50 islets/mouse, analyzed in a blinded fashion). Values are presented as the average surface area per islet ± SEM.

Increased levels of oxidized protein in islets of $Hfe^{-/-}$ mice

We next determined whether islets isolated from $Hfe^{-/-}$ mice exhibited markers of increased cellular oxidative stress. Protein modification by carbonyl groups was assessed in islets from wild-type and $Hfe^{-/-}$ mice. Densitometric quantification of protein immunoblots revealed a significant increase of 58% in the density of total carbonyl protein modifications in islets from $Hfe^{-/-}$ mice (Fig. 6; $P < 0.01$).

Normal glucose tolerance despite decreased insulin secretory capacity in $Hfe^{-/-}$ mice

Mice of 10 wk of age were next examined for any loss of glucose tolerance associated with the decrease in islet insulin content. The $Hfe^{-/-}$ and $Hfe^{+/+}$ mice did not differ in weight (21.3 ± 0.5 g for $Hfe^{-/-}$ and 20.6 ± 0.7 for $Hfe^{+/+}$; not significantly different). Fasting glucose levels were slightly elevated in the $Hfe^{-/-}$ (100 ± 3 mg/dl for $Hfe^{-/-}$ and 86 ± 2 for $Hfe^{+/+}$; $P < 0.001$; Fig. 7A). Surprisingly, however, the $Hfe^{-/-}$ mice had no impairment in glucose tolerance compared with wild-type controls, with significantly lower blood glucose values 60 and 120 min after an ip glucose challenge (1 mg/g body weight; Fig. 7A). The overall area under the glucose curve was 14% lower in $Hfe^{-/-}$ mice compared with controls ($P < 0.05$; Fig. 7B). The incremental area under the glucose curve was decreased by 52% in the $Hfe^{-/-}$ mice compared with controls (7927.8 ± 476 mg/min·dl for $Hfe^{+/+}$ and 3772 ± 226 mg/ min·dl for $Hfe^{-/-}$; $P < 0.001$; n = 21 mice/group; not shown). Fasting serum insulin levels were comparable in $Hfe^{-/-}$ and $Hfe^{+/+}$ mice (Fig. 7C; 17% lower in $Hfe^{-/-}$; nonsignificantly different, $P = 0.18$). Insulin levels at 30 min were 48% lower in $Hfe^{-/-}$ mice ($P = 0.001$). Abnormal glucose tolerance did not develop in male or female mice as old as 12–14 months, even with additional iron loading by dietary iron or ip iron-dextran (not shown). Insulin tolerance testing revealed no significant differences in insulin sensitivity for blood glucose levels between the $Hfe^{-/-}$ mice and the wild-type controls (Fig. 7D).

Decreased insulin secretion and insulin content, but normal glucose tolerance, in two other models of iron overload

We next examined two other models of iron overload in mice. In the first model, mice harbor a mutation in the *Hfe* gene that results in the equivalent C282Y mutation found in the majority of hereditary hemochromatosis in humans ($Hfe^{y/y}$). In the second, iron overload was induced by main-

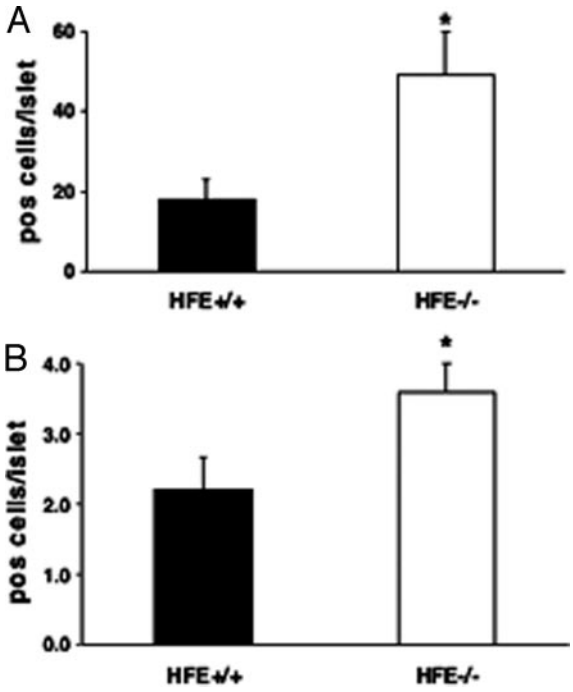

FIG. 4. Increased apoptosis in islets of $Hfe^{-/-}$ mice. A, Increased numbers of β-cells with activated caspase 3 in $Hfe^{-/-}$ mice (48.8 ± 10.8 cells/islet for $Hfe^{-/-}$ *vs.* 18.2 ± 4.8 for controls; *, $P < 0.03$). B, Increased numbers of TUNEL-positive β-cells in $Hfe^{-/-}$ mice (3.6 ± 0.4 cells/islet for $Hfe^{-/-}$ *vs.* 2.2 ± 0.5 for controls; mice were 8–10 months old; *, $P = 0.05$).

taining mice on a diet supplemented with carbonyl iron. Like $Hfe^{-/-}$ mice, neither $Hfe^{y/y}$ mice nor mice fed excess dietary iron displayed abnormal glucose tolerance after IPGTT (Fig. 8A) despite significantly decreased insulin/glucose ratios (Fig. 8B). The islet insulin content was decreased in the $Hfe^{y/y}$ mice to a level 54 ± 3% of that in controls ($P < 0.05$; data not shown), and islet iron content was 1.42-fold higher ($P < 0.05$; data not shown). The latter two parameters were not determined in the iron-fed group.

Age-dependent decrease in glucose tolerance in C57BL6 $Hfe^{-/-}$ mice

To determine whether diabetes would develop with hemochromatosis in a strain more susceptible to diabetes, we cross-bred the $Hfe^{-/-}$ mice onto the C57BL6 background for at least eight generations to generate C57BL6 $Hfe^{-/-}$ mice. We examined these mice for changes in glucose tolerance associated with aging. C57BL6 $Hfe^{-/-}$ mice did not normally compensate for aging with hyperinsulinemia, as demonstrated by the reduced fasting insulin levels in mice 10–12 months of age (Fig. 9A). This inability to increase insulin levels with age was associated with a modest decrement in glucose tolerance in the C57BL6 $Hfe^{-/-}$ mice compared with their age-matched, wild-type counterparts (Fig. 9B).

Discussion

We have demonstrated that iron overload induced by targeted inactivation of the *Hfe* gene in mice results in decreased insulin secretory capacity. This decrease is due to apoptosis

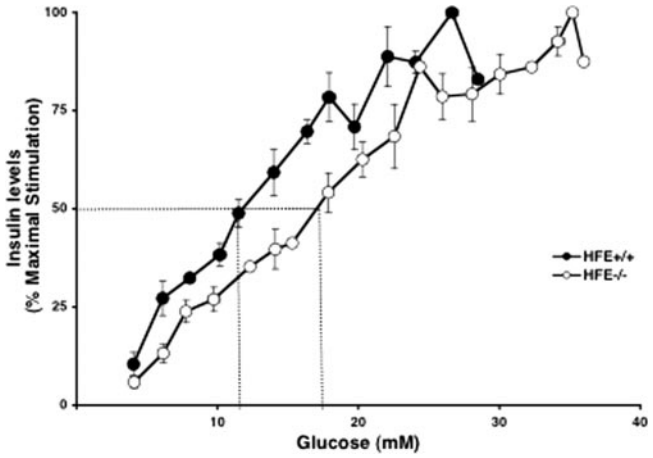

FIG. 5. Compromised glucose sensing in islets of $Hfe^{-/-}$ mice. Islets isolated from 8- to 10-month-old control (○) or $Hfe^{-/-}$ (●) mice were perifused for 30 min in basal medium containing 3 mM glucose at a flow rate of 1 ml/min at 37 C before collection of fractions. Glucose concentrations were increased gradually as indicated. Fractions of the perifusing buffer were collected at 1-min intervals, and glucose and insulin contents were measured. Insulin secretion is presented as a percentage of maximal stimulation. Isolated islets from $Hfe^{-/-}$ mice required significantly higher glucose concentration (16.68 ± 0.87 *vs.* 13.1 ± 0.62 mM glucose; n = 7 for wild-type mice and n = 6 for $Hfe^{-/-}$ mice; $P < 0.006$) for half-maximal stimulation. The actual maximal levels of insulin secretion were 283 ± 43 pg/islet in wild-type islets compared with 241 ± 31 pg/islet in $Hfe^{-/-}$ mice (not shown).

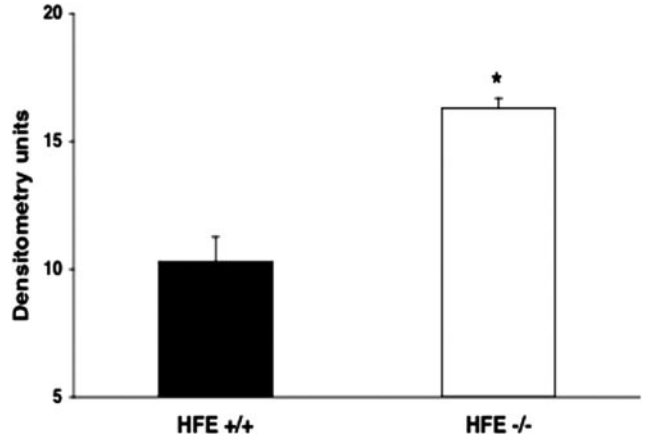

FIG. 6. Increased levels of oxidized proteins in islets of $Hfe^{-/-}$ mice. The carbonyl content of total protein from homogenized islets of $Hfe^{+/+}$ control and $Hfe^{-/-}$ mice was assessed by immunoblotting with specific antibodies (not shown). Arbitrary densitometric units are the mean ± SEM, showing increased content of oxidized carbonyl proteins (*, $P < 0.01$) in islets from $Hfe^{-/-}$ mice compared with islets from $Hfe^{+/+}$ control mice (n = 5 separate pancreata each from $Hfe^{-/-}$ and $Hfe^{+/+}$ mice; mice were 8–10 months old).

and loss of pancreatic islet size and is associated with increased markers of oxidative stress in the affected islets, as might be expected if the initiating factor is excess iron. Indeed, the similarity of the phenotypes in $Hfe^{-/-}$, mice bearing the mutation found in the majority of human hemochromatosis ($Hfe^{y/y}$), and mice fed excess dietary iron suggests that β-cell failure and β-cell apoptosis are a direct result of iron toxicity. The basis for the sensitivity of the β-cell, in particular, to iron is not completely understood. One possibility is

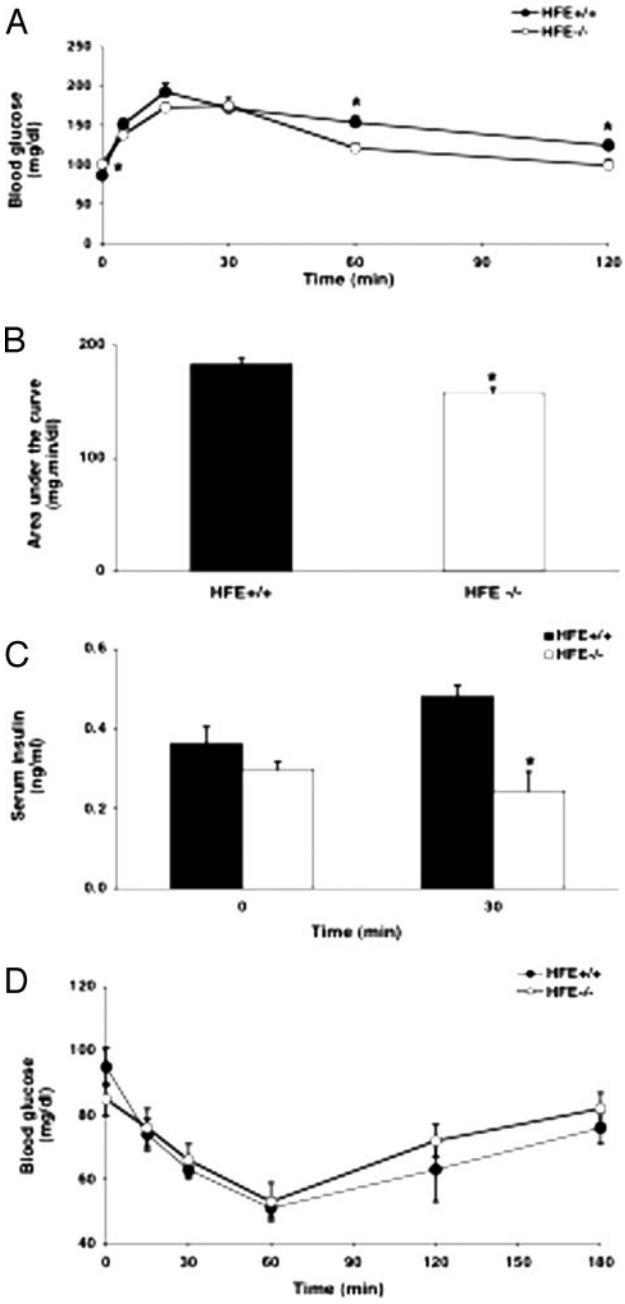

FIG. 7. Glucose and insulin tolerance analyses. A, Glucose (1 mg/g body weight) was ip administered in $Hfe^{-/-}$ and control mice, and tail vein glucose levels were determined at the indicated times (n = 8 control and n = 9 $Hfe^{-/-}$; *, $P < 0.05$ for $Hfe^{-/-}$ compared with $Hfe^{+/+}$ controls). B, Total area under the glucose curve for the data shown in A (*, $P < 0.05$). C, Insulin levels were determined before and 30 min after glucose injection in the same cohort (*, $P < 0.001$). D, Insulin (0.75 U/kg body weight) was administered ip, and blood glucose levels were determined at the indicated times (n = 6). Data are the mean ± SEM.

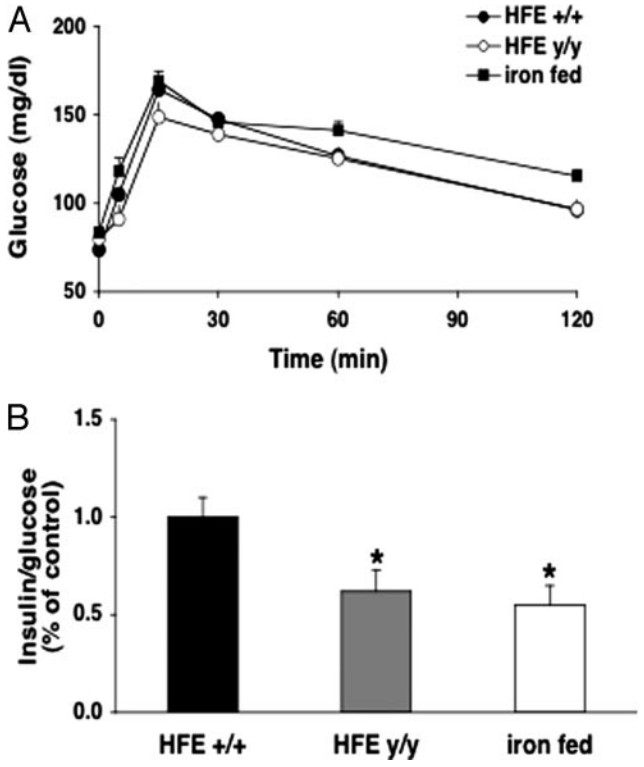

FIG. 8. Normal glucose tolerance (A), but decreased insulin secretory capacity (B), in $Hfe^{y/y}$ mice and in mice fed excess dietary carbonyl iron (n = 8–10 mice/group; 6–8 months old; *, $P < 0.05$).

that the β-cell simply accumulates more iron than other cells, based on relatively high levels of expression of transmembrane divalent metal transporters (16) needed to facilitate zinc uptake for packaging insulin in secretory granules. The high saturation of transferrin, which is the phenotypic hallmark of hemochromatosis, is associated with the presence of nontransferrin-bound iron in plasma, and nontransferrin-bound iron is readily taken up by cells via divalent metal transporter-1 (17, 18). Potentially high iron fluxes through this pathway might explain the high levels of apo-ferritin in normal β-cells (19). The β-cell may also be particularly susceptible to oxidative damage, perhaps based on the nearly exclusive reliance upon mitochondrial metabolism of glucose for glucose-induced insulin secretion. Oxidative damage to mitochondria may explain both the impairment of glucose sensing for insulin secretion as well as subsequent apoptosis.

Part of the classic clinical description of human hemochromatosis is diabetes, but the true prevalence of diabetes and the relative contributions to that diabetes of insulin secretory defects, insulin resistance, and altered glucose production by the liver have not been systematically examined. One study of human subjects with hemochromatosis demonstrated a significant decrease in the acute insulin response to glucose (AIRg) during an iv glucose tolerance test (20), but this was true in subjects both with and without diabetes. Reduction of iron stores by phlebotomy increased the AIRg by 35%. Similar impairment of the β-cell response in the face of iron overload has been seen in patients with thalassemia major (21) and in rats subjected to experimental iron overload (8). Other studies have demonstrated insulin resistance in subjects with diabetes and hemochromatosis (22), particularly in the presence of hepatic disease (23), and phlebotomy can result in improved insulin sensitivity (24).

The mouse models of hemochromatosis, like many humans with the disease, do not develop diabetes despite de-

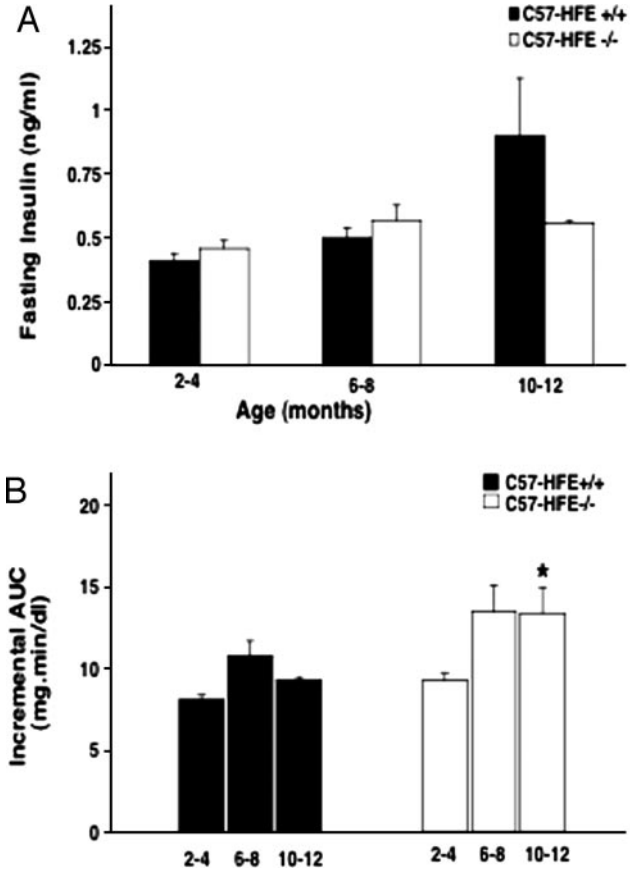

FIG. 9. Fasting insulin levels and glucose tolerance analyses in C57BL6 mice. A, Fasting insulin levels were analyzed in C57BL6 $Hfe^{-/-}$ and C57BL6 $Hfe^{+/+}$ control mice at the indicated ages (n = 3–17/group/strain; all male). B, Glucose (1 mg/g body weight) was ip administered to C57BL6 $Hfe^{-/-}$ and control mice. Tail vein glucose levels were determined at the indicated ages, and the incremental area under the curve was determined (n = 3–19/group/strain; *, $P < 0.05$ for $Hfe^{-/-}$ compared with $Hfe^{+/+}$ controls. Data are the mean ± SEM.

creased insulin secretory capacity. This is true in both the 129/Sv and the more diabetes-prone C57BL6 strains, although in the latter, a modest degree of glucose intolerance did develop with aging. There are several possible explanations for this. First, there may simply be a quantitative requirement for more time or more iron overload to lead to loss of a critical mass of β-cells. We have followed mice for up to 14 months, and we have fed $Hfe^{-/-}$ mice excess carbonyl iron or injected iron dextran ip to accentuate the iron overload, but in none of these cases has diabetes developed (not shown). These maneuvers do not rule out the possibility that a critical threshold of iron-induced damage still has not been reached. In surgical pancreatectomy models, resection of 85–95% of the pancreas is generally required to reproducibly induce hyperglycemia in the short term (25). Resection of 70–85% of the pancreas results in hyperglycemia in a period of weeks (26), and up to 50% resection is generally well tolerated in an otherwise metabolically normal individual (27). Of note, however, older $Hfe^{-/-}$ mice did exhibit normal glucose homeostasis despite chronic decreases in insulin levels after glucose challenge of up to 68% (not shown), close to the threshold of the 70% loss of insulin that can result in diabetes.

Another possible explanation for the failure to develop diabetes is that a second insult to the organs involved in fuel homeostasis is needed. That is, with the levels of iron overload found in typical hemochromatosis, it may be unusual to develop diabetes purely on the basis of decreased insulin secretion. If, however, insulin resistance were to develop concomitantly with the insulin secretory defect, diabetes might result. Consistent with this, the $Hfe^{-/-}$ mice were not insulin resistant, as evidenced by normal insulin testing. There is evidence to support the hypothesis that insulin resistance may be needed in hemochromatosis before diabetes will develop. For example, insulin resistance can be seen in subjects with diabetes resulting from hemochromatosis (22, 23) or iron overload (24). The origin of this insulin resistance may be multifactorial. Insulin resistance is a hallmark of typical type 2 diabetes (28–30), and it is possible that those individuals with hemochromatosis who develop diabetes are those who are also genetically at risk for type 2 diabetes. In fact, if type 2 diabetes is a disease that results when insulin resistance is no longer compensated because of β-cell failure (28), one would predict that in kindreds with both hemochromatosis and typical type 2 diabetes, the "built-in" β-cell insufficiency resulting from hemochromatosis might result in earlier and/or more severe presentations of type 2 diabetes.

Another potential mechanism for insulin resistance and progression to diabetes in individuals with hemochromatosis is iron-induced liver damage. This possibility is supported by the known relationship between diabetes and cirrhosis of any etiology. For example, there is a 24% prevalence of diabetes in cirrhotic subjects with hepatitis C, whereas hepatitis without cirrhosis is not associated with diabetes (31). Fasting insulin levels in the cirrhotic subjects with diabetes are significantly elevated, consistent with a major role for insulin resistance in the diabetic phenotype (31). Treatment of hepatitis C with interferon improves insulin sensitivity by nearly 3-fold, but does not affect insulin secretion (32). The relationship between diabetes and hepatic damage in hemochromatosis is also supported by our review of records of individuals with hemochromatosis. Of 104 clinically affected male probands, 32 (31%) had diabetes, and of these, 23 had biopsy-proven cirrhosis, five had moderate fibrosis, and only four had normal liver architecture (Kushner, J. P., unpublished observations). Thus, the failure of $Hfe^{-/-}$ mice to progress to diabetes may be related to the fact that these mice do not develop cirrhosis or significant liver disease (Ajioka, R., and J. P. Kushner, unpublished observations).

An interesting observation made in these studies is that insulin deficiency is compensated and does not result in significant glucose intolerance. We have observed the same phenomenon in humans with hemochromatosis. Although other studies have demonstrated insulin resistance with hemochromatosis after the onset of diabetes (21, 22), when these individuals are studied before the onset of diabetes, there is a decrease in AIRg that is nearly fully compensated by increased insulin sensitivity (McClain, D., J. Kushner, and D. Abraham, manuscript in preparation). It is known that organisms respond to hyperinsulinemia by compensatory decreases in insulin sensitivity (33–36), and the converse (increased insulin sensitivity with hypoinsulinemia) has been observed in animal models (37). The basis for this in-

crease in insulin sensitivity is currently under study and may involve decreased adiposity resulting from hypoinsulinemia. Hepatic glucose production may also be dysregulated because of hepatic iron overload, although fasting glycemia and responses to prolonged fasting (not shown) are not markedly different in $Hfe^{-/-}$ mice.

In summary, we report that iron overload in mouse models of hemochromatosis results in a loss of insulin secretory capacity, but that this defect by itself is insufficient to cause diabetes mellitus. The results have several implications for human disease and our understanding of more common forms of diabetes. The data support a primary pathogenic role for iron in the β-cell and the desirability of early detection and treatment of iron overload in humans before irreversible damage to the β-cell or liver results (6, 21).

Acknowledgments

Received March 25, 2004. Accepted August 4, 2004.

Address all correspondence and requests for reprints to: Dr. Donald A. McClain, Division of Endocrinology, University of Utah School of Medicine, 30 North 2030 East, Salt Lake City, Utah 84132. E-mail: donald.mcclain@hsc.utah.edu.

This work was supported by the Research Service of the Veterans Administration, National Institutes of Health Grant DK59512, and the Ben and Iris Margolis Foundation.

R.C.C. and H.A.J. contributed equally to this work.

References

1. **Edwards C** 1999 Hemochromatosis. In: Lee GR, Foerster J, Lukens J, Paraskevas F, Greer JP, Rodgers GM, eds. Wintrobe's clinical hematology. Baltimore: Williams & Wilkins; 1056–1070
2. **Bothwell TH, Charlton R, Motulsky AG** 1995 Hemochromatosis. In: Scriver CR, Beaudet A, Sly WS, Valle D, eds. The metabolic and molecular bases of inherited disease. New York: McGraw-Hill; 2237–2269
3. **Feder JN, Tsuchihashi Z, Irrinki A, Lee VK, Mapa FA, Morikang E, Prass CE, Starnes SM, Wolff RK, Parkkila S, Sly WS, Schatzman RC** 1997 The hemochromatosis founder mutation in HLA-H disrupts β_2-microglobulin interaction and cell surface expression. J Biol Chem 272:14025–14028
4. **Feder JN, Penny DM, Irrinki A, Lee VK, Lebron JA, Watson N, Tsuchihashi Z, Sigal E, Bjorkman PJ, Schatzman RC** 1998 The hemochromatosis gene product complexes with the transferrin receptor and lowers its affinity for ligand binding. Proc Natl Acad Sci USA 95:1472–1477
5. **Edwards CQ, Dadone MM, Skolnick MH, Kushner JP** 1982 Hereditary haemochromatosis. Clin Haematol 11:411–435
6. **Bulaj ZJ, Ajioka RS, Phillips JD, LaSalle BA, Jorde LB, Griffen LM, Edwards CQ, Kushner JP** 2000 Disease-related conditions in relatives of patients with hemochromatosis. N Engl J Med 343:1529–1535
7. **Levy JE, Montross LK, Cohen DE, Fleming MD, Andrews NC** 1999 The C282Y mutation causing hereditary hemochromatosis does not produce a null allele. Blood 94:9–11
8. **Pelot D, Zhou XJ, Carpenter P, Vaziri ND** 1998 Effects of experimental hemosiderosis on pancreatic tissue iron content and structure. Dig Dis Sci 43: 2411–2414
9. **Brandhorst H, Brandhorst D, Brendel MD, Hering BJ, Bretzel RG** 1998 Assessment of intracellular insulin content during all steps of human islet isolation procedure. Cell Transplant 7:489–495
10. **Zawalich WS, Diaz VA, Zawalich KC** 1988 Role of phosphoinositide metabolism in induction of memory in isolated perifused rat islets. Am J Physiol 254:E609–E616
11. **Zawalich WS, Bonnet-Eymard M, Zawalich KC** 1998 Glucose-induced desensitization of the pancreatic β-cell is species dependent. Am J Physiol 275: E917–E924
12. **Edwards CQ, Carroll M, Bray P, Cartwright GE** 1977 Hereditary hemochromatosis. Diagnosis in siblings and children. N Engl J Med 297:7–13
13. **Labat-Moleur F, Guillermet C, Lorimier P, Robert C, Lantuejoul S, Brambilla E, Negoescu A** 1998 TUNEL apoptotic cell detection in tissue sections: critical evaluation and improvement critical evaluation and improvement. J Histochem Cytochem 46:327–334
14. **Kulkarni RN, Wang ZL, Wang RM, Hurley JD, Smith DM, Ghatei MA, Withers DJ, Gardiner JV, Bailey CJ, Bloom SR** 1997 Leptin rapidly suppresses insulin release from insulinoma cells, rat and human islets and, in vivo, in mice. J Clin Invest 100:2729–2736
15. **Morrison TB, Weis JJ, Wittwer CT** 1998 Quantification of low-copy transcripts by continuous SYBR Green I monitoring during amplification. Biotechniques 24:954–958, 960–962
16. **Andrews NC** 1999 The iron transporter DMT1. Int J Biochem Cell Biol 31: 991–994
17. **Kaplan J, Jordan I, Sturrock A** 1991 Regulation of the transferrin-independent iron transport system in cultured cells. J Biol Chem 266:2997–3004
18. **Sturrock A, Alexander J, Lamb J, Craven CM, Kaplan J** 1990 Characterization of a transferrin-independent uptake system for iron in HeLa cells. J Biol Chem 265:3139–3145
19. **MacDonald MJ, Cook JD, Epstein ML, Flowers CH** 1994 Large amount of (apo)ferritin in the pancreatic insulin cell and its stimulation by glucose. FASEB J 8:777–781
20. **Hramiak IM, Finegood DT, Adams PC** 1997 Factors affecting glucose tolerance in hereditary hemochromatosis. Clin Invest Med 20:110–118
21. **Mangiagli A, Italia S, Campisi S** 1998 Glucose tolerance and β-cell secretion in patients with thalassaemia major. J Pediatr Endocrinol Metab 11:985–986
22. **Dymock IW, Cassar J, Pyke DA, Oakley WG, Williams R** 1972 Observations on the pathogenesis, complications and treatment of diabetes in 115 cases of haemochromatosis. Am J Med 52:203–210
23. **Niederau C** 1999 Diabetes mellitus in hemochromatosis. Z Gastroenterol (Suppl 1):22–32
24. **Facchini FS** 1998 Effect of phlebotomy on plasma glucose and insulin concentrations. Diabetes Care 21:2190
25. **Laybutt DR, Glandt M, Xu G, Ahn YB, Trivedi N, Bonner-Weir S, Weir GC** 2003 Critical reduction in β-cell mass results in two distinct outcomes over time. Adaptation with impaired glucose tolerance or decompensated diabetes. J Biol Chem 278:2997–3005
26. **Yasugi H, Mizumoto R, Sakurai H, Honjo I** 1976 Changes in carbohydrate metabolism and endocrine function of remnant pancreas after major pancreatic resection. Am J Surg 132:577–580
27. **Robertson RP, Lanz KJ, Sutherland DE, Seaquist ER** 2002 Relationship between diabetes and obesity 9 to 18 years after hemipancreatectomy and transplantation in donors and recipients. Transplantation 73:736–741
28. **Olefsky JM** 1993 Insulin resistance and the pathogenesis of non-insulin dependent diabetes mellitus: cellular and molecular mechanisms. Adv Exp Med Biol 334:129–150
29. **Laws A, Stefanick ML, Reaven GM** 1989 Insulin resistance and hypertriglyceridemia in nondiabetic relatives of patients with noninsulin-dependent diabetes mellitus. J Clin Endocrinol Metab 69:343–347
30. **Sakul H, Pratley R, Cardon L, Ravussin E, Mott D, Bogardus C** 1997 Familiality of physical and metabolic characteristics that predict the development of non-insulin-dependent diabetes mellitus in Pima Indians. Am J Hum Genet 60:651–656
31. **Caronia S, Taylor K, Pagliaro L, Carr C, Palazzo U, Petrik J, O'Rahilly S, Shore S, Tom BD, Alexander GJ** 1999 Further evidence for an association between non-insulin-dependent diabetes mellitus and chronic hepatitis C virus infection. Hepatology 30:1059–1063
32. **Konrad T, Zeuzem S, Vicini P, Toffolo G, Briem D, Lormann J, Herrmann G, Berger A, Kusterer K, Teuber G, Cobelli C, Usadel KH** 2000 Evaluation of factors controlling glucose tolerance in patients with HCV infection before and after 4 months therapy with interferon-α. Eur J Clin Invest 30:111–121
33. **Del Prato S, Riccio A, Vigili de Kreutzenberg S, Dorella M, Avogaro A, Marescotti MC, Tiengo A** 1993 Mechanisms of fasting hypoglycemia and concomitant insulin resistance in insulinoma patients. Metabolism 42:24–29
34. **Rizza RA, Mandarino LJ, Genest J, Baker BA, Gerich JE** 1985 Production of insulin resistance by hyperinsulinaemia in man. Diabetologia 28:70–75
35. **Miles PD, Li S, Hart M, Romeo O, Cheng J, Cohen A, Raafat K, Moossa AR, Olefsky JM** 1998 Mechanisms of insulin resistance in experimental hyperinsulinemic dogs. J Clin Invest 101:202–211
36. **Tang J, Neidigh JL, Cooksey RC, McClain DA** 2000 Transgenic mice with increased hexosamine flux specifically targeted to β-cells exhibit hyperinsulinemia and peripheral insulin resistance. Diabetes 49:1492–1499
37. **Minami A, Iseki M, Kishi K, Wang M, Ogura M, Furukawa N, Hayashi S, Yamada M, Obata T, Takeshita Y, Nakaya Y, Bando Y, Izumi K, Moodie SA, Kajiura F, Matsumoto M, Takatsu K, Takaki S, Ebina Y** 2003 Increased insulin sensitivity and hypoinsulinemia in APS knockout mice. Diabetes 52:2657–2665